Effects of tephra falls on vegetation: A Late-Quaternary record from southern Italy

Judy R.M. Allen and Brian Huntley*

Department of Biosciences, Durham University, South Road, Durham DH1 3LE, United Kingdom

* Corresponding author

e-mail: brian.huntley@durham.ac.uk

Tel: +44 (0)191 334 1282

Running headline: **Effects of tephra falls on vegetation**

Summary

1. Impacts of tephra deposition on vegetation are recorded in a series of ten high temporal resolution absolute pollen diagrams from Lago Grande di Monticchio, each diagram spanning a single tephra deposition event during the last glacial–interglacial cycle.
2. Sediment accumulation rates determined by counting and measurement of annual laminations ('varves') provide an accurate and precise chronology, enabling the minimum recovery time after a tephra fall to be determined.
3. In most cases pollen accumulation rate was reduced after the tephra fall, indicating reduced vegetation productivity. Tephra deposition events also led to changes in vegetation composition, although these varied in magnitude.
4. The magnitude and duration of the impacts upon the vegetation were related to the thickness of the tephra layer deposited, the thickest layers examined (>250 mm) having minimum recovery times of up to a century and thicker layers generally having greater impacts upon pollen productivity and vegetation composition.
5. Tephra chemistry also influenced the persistence of the impact.
6. The nature of the prevailing vegetation prior to the tephra fall influenced the degree and persistence of the impact. Tephra layers <30 mm thick had minimum recovery times of up to 90 years when they fell on wooded steppe vegetation, whereas cold steppe recovered much more quickly, as did forest.
7. The relative sensitivity of wooded steppe was contrary to our expectations.
8. Of individual pollen taxa, Cupressaceae emerged as particularly sensitive to tephra deposition.

Synthesis – Applying absolute pollen analytical methods to a sediment record with a well-supported and precise chronology obtained from a lake in a volcanic region where the vegetation has been subject to numerous tephra deposition events enabled us to explore the impacts of such events. Our results provide evidence of differential impacts upon individual plant taxa and of differential sensitivity of three vegetation types that have prevailed in the region during the last glacial–interglacial cycle. The influences of tephra thickness and chemistry on minimum recovery time were substantial. Our results are relevant to forecasting the potential impacts upon ecosystems of volcanic eruptions.

Tweetable Abstract

Impacts of tephra falls on vegetation depend upon tephra thickness and chemistry, and the prevailing vegetation.

Key Words

Absolute pollen analysis

Cold steppe

Forest

High temporal resolution

Lago Grande di Monticchio

Last glacial–interglacial cycle

Plant population and community dynamics

Tephra thickness

Tephra chemistry

Wooded steppe

Introduction

In the many regions of the world with active volcanoes, vegetation faces various hazards arising from volcanic eruptions (Lees and Neall, 1993). In areas proximal to an erupting volcano, vegetation is subject to direct physical disruption by phenomena such as lava or pyroclastic flows that may emanate from that volcano and spread across the surrounding landscape. The vegetation of much larger areas, however, faces various hazards arising from the episodic deposition of tephra ('volcanic ash') (Arnalds, 2013). Tephra is ejected explosively during volcanic eruptions and dispersed in the atmosphere to varying distances, principally according to the size of the tephra particles. Following large eruptions, tephra falls of considerable depth can blanket the landscape for distances of a hundred kilometres or more downwind from the source. The Mazama tephra of north-west North America, for example, derived from the climactic eruption of Mount Mazama 7627 ± 150 cal B.P. (Zdanowicz et al., 1999) that resulted in the caldera now occupied by Crater Lake, Oregon, forms a layer *ca*. 400 mm thick at a distance of 200 km from the source and is still 40–50 mm thick at 1000 km (Hoblitt et al., 1987). Finer tephra particles can travel very long distances, giving rise to so-called 'cryptotephra' layers that are not visible to the naked eye but that can provide valuable age markers in peats and lake sediments (Turney et al., 2004), some of which can potentially be useful at hemispheric extents (e.g. the White River Ash erupted from a volcano in Alaska has been found at distances of >7000 km in Ireland and other parts of northern Europe, Jensen et al., 2014). Not only do falls of tephra bury and potentially kill vegetation, but the physical characteristics, pH and chemical composition of the tephra can strongly influence the nature and extent of the impact upon vegetation, as well as its subsequent recovery (Hotes et al., 2010). Bulk atmospheric wet and/or dry deposition of major cations and anions, the latter including especially fluorine, chlorine and sulphur (Aiuppa et al., 2006), from the volcanic plume can further impact upon vegetation (e.g. Bellomo et al., 2007).

Where trees are a component of vegetation, tephra may accumulate on their foliage; such accumulations will impair the functioning of leaves and potentially damage them or even cause extensive defoliation, in turn possibly leading to longer-term damage to, or even death of, the trees. Del Moral and Grishin (1999) report results of observations of the impacts upon vegetation of tephra deposited by the 1907 eruption of the Ksudach volcano, Kamchatka, and the pattern of vegetation recovery over the subsequent 90-year interval. They report that tephra accumulations of >700 mm killed all vegetation,

including trees, although with dead tree remains typically emerging where the depth was less than 1000 mm; subsequent recovery in such areas was by primary succession on the tephra surface and had progressed only as far as occurrences of lichen mats and scattered herbs after 90 years, thus likely requiring a period of several centuries before a tree canopy would be reinstated. Shallower accumulations allowed survival of isolated trees, but survival of a majority of trees was seen only with accumulations <300 mm. Tephra accumulations of 200–300 mm in open areas or beneath trees smothered lower growing vegetation, killing dwarf shrubs as well as herbaceous taxa and cryptogams (del Moral and Grishin, 1999). Dwarf-shrubs and herbaceous taxa were damaged but not killed by accumulations of <200 mm, but bryophytes and lichens survived only where tephra depth was <100 mm. In a similar study of the impacts of tephra accumulations following the 1980 eruption of Mount St. Helens, Washington, USA, Zobel and Antos (1997) showed a substantial proportion of herbaceous taxa were killed in plots where the accumulation was > 100 mm. The same workers subsequently showed that even where <50 mm of tephra had accumulated, forest understorey vegetation was still different from its pre-eruption state after 20 years (Antos and Zobel, 2005), and that after 33 years vegetation patches that received shallow deposits of tephra, insufficient to bury the plants, diverged more from patches where no tephra fell than they had done only two years after the eruption (Fischer et al., 2016).

The impacts of tephra on vegetation have also been investigated using field experiments (see e.g. Hotes et al., 2010, Hotes et al., 2004, Payne and Blackford, 2005). Although the results have not always been consistent, they provide evidence that the chemical and physical properties of the tephra, as well as its thickness, together determine the extent of the impact upon vegetation. Palaeovegetation, principally palynological, data too have been used to investigate the impacts of tephra falls, once again with apparently inconsistent results. Birks and Lotter (1994) explored the impact of the Laacher See tephra, deposited *ca*. 11,000 B.P., on the vegetation around three lakes at varying distances from the eruption, finding a significant effect only at the closest lake, 60 km from the eruption, where the tephra layer was 80 mm thick. Following the eruption the proportion of non-arboreal pollen at this site, principally Poaceae, was increased for a period of *ca*. 20 years. Charman *et al*. (1995) examined the evidence for the impacts of three Icelandic tephras deposited in a peat profile in northern Scotland, finding evidence that the two older tephra deposition events impacted upon the vegetation, but that the third had no apparent impact. Whereas the oldest tephra, dated to *ca*. 7650 B.P., was associated with a decrease in relative abundance

of pollen derived from trees and shrubs and a parallel increase in Cyperaceae pollen, the second layer, dated to *ca*. 4250 B.P. and likely to be derived from the Hekla 4 eruption, coincided with a short-lived peak in pollen of *Pinus*. This latter peak, however, has been shown to be time-transgressive across northern Scotland (Daniell, 1997, Huntley et al., 1997); *Pinus* pollen abundance peaked significantly before deposition of the Hekla 4 tephra at sites further south and west, termination of the peak coinciding with the tephra only at sites to the north-east (Blackford et al., 1992). As Gear and Huntley (1991) hypothesised, the short-lived expansion and subsequent decline of *Pinus* in northern Scotland most likely reflects a climatic fluctuation, the association with the Hekla 4 tephra at some localities being purely coincidental. In contrast to the foregoing studies, an investigation of the potential impact of tephra deposited in a Turkish lake, Gölhisar, following the powerful eruption of Santorini *ca*. 3300 B.P. found no significant impacts on terrestrial vegetation (Eastwood et al., 2002). Similarly, Egan *et al*. (2016) found no evidence of an impact upon the regional forest vegetation of any of three tephra deposition events, including a 30 mm thick layer derived from the climactic eruption of Mount Mazama, at Moss Lake in the northern Cascades, Washington. Further south, however, in Oregon, in four lakes where the main Mazama tephra layer is between 140 mm and 500 mm thick, Long *et al*. (2014) report no impact upon the taxonomic composition of the vegetation but a relatively short-lived, 50 – 100 year, negative impact upon the pollen productivity of non-woody taxa at three of the lakes investigated, resulting in a temporary decrease in relative abundance of non-arboreal pollen.

In addition to their potential direct impacts upon vegetation, both relatively thick and thinner (< 100 mm) tephra accumulations also may have short- or long-term effects upon soil chemistry, the exact nature of which will depend upon the chemical properties of the tephra. Soil fertility may be increased or decreased, whilst some tephras may cause soil acidification and/or contain elements that are toxic to most plants (Payne and Blackford, 2005). In some cases the altered soil chemistry may itself cause death even of trees and other long-lived plants (Wilmshurst and McGlone, 1996). Deeper accumulations (> *ca*. 200 mm) provide a new surface upon which ecological succession takes place, leading to pedogenesis within the deposit. In regions subject to repeated episodes of tephra deposition the resulting disturbances to the vegetation may be important in determining vegetation dynamics and potentially also vegetation structure (Horrocks and Ogden, 1998).

Southern Italy is a region with many active or recently active volcanoes (Fig. 1) where numerous explosive eruptions have occurred, resulting in repeated episodes of tephra deposition and the potential for resultant disruption of ecosystems. Most Italian volcanoes have been active during the last glacial–interglacial cycle, particularly those of the Campanian Province. Highly explosive eruptions of Vesuvius, the Phlegrean Fields, Ischia, Procida-Vivara, the Aeolian Islands, Etna and Pantelleria (see Fig. 1) all have occurred during the late Pleistocene, with the first four of these in particular producing numerous tephra layers during this time (Wulf et al., 2004). There have been *ca*. 72 eruptions in the Phlegrean Fields, for example, since *ca*. 14 ka BP. Most Italian volcanoes produce andesitic tephra shards that are characteristically relatively rich in potassium (Wulf et al., 2004, and see Supplementary Information Table S1). Although only a limited number of studies report investigations of pedogenesis on Italian tephra deposits (see e.g. Colombo et al., 2014, Ermice, 2017, Scarciglia et al., 2014, Vacca et al., 2003), these studies suggest that pedogenesis is often more strongly influenced by the prevailing climate than by the character of the tephra, although there is evidence that more clay-rich soils may develop on finer more distal tephras.

Southern Italy also has a number of lakes occupying volcanic craters. The sediments accumulated within these maar lakes preserve records both of tephra deposition and of the vegetation. Lago Grande di Monticchio (LGdM; 40° 56′ 40″ N, 15° 36′ 30″ E, 656 m above sea level, Fig. 1) is one such maar lake that lies generally downwind of Italian volcanoes active during the late Pleistocene and where previous investigations have shown the presence of numerous tephra layers of varying thickness (Narcisi, 1996, Wulf, 2000, Wulf et al., 2004, 2006), as well as of well-preserved pollen (see e.g. Allen et al., 2000, 2002, Allen and Huntley, 2009) (Fig. 2), in the 102·3 m thick sediment sequence. In addition, the sediments deposited in this lake are in large part annually laminated, allowing a detailed independent chronology to be developed (Zolitschka and Negendank, 1996, Brauer et al., 2007) establishing that they extend back to at least 132·9 ka BP. They thus extend from the penultimate glacial stage through the last glacial–interglacial cycle in its entirety and up to the present. During this time the structure and composition of the vegetation of the surrounding region has ranged between predominantly mesic forest, especially during the last interglacial and Holocene, more boreal woodlands and wooded steppe, during last glacial interstadials, xeric woodlands, especially during the early part of the last interglacial and the late Holocene, and arid cold steppe, during last glacial stadials and the later part of the penultimate glacial stage.

Taking advantage of the unique features of the record from LGdM, our study aimed to explore the nature and persistence of the impacts of episodes of tephra deposition upon the vegetation of the surrounding region. Using fine temporal resolution pollen analysis of the sediments immediately below and above a series of tephra layers (e.g. TM-24a, Fig. 3), we explored the impacts of tephras of a range of thicknesses and varying chemistry that were deposited during periods of different predominant vegetation on the surrounding landscape. We expected tephra deposition to result in changes in either or both of the structure and composition of the vegetation, both of which the pollen analytical data would record. We also expected thicker tephra layers to have greater and more persistent impacts upon the vegetation, but that this would be modulated by the character of the vegetation prior to tephra deposition. Thus a given thickness of tephra might have a greater and more enduring impact upon herb-dominated vegetation than upon forest vegetation. We also expected the varying chemistry of tephra layers potentially to influence the strength and nature of their impact upon the vegetation.

Materials and Methods

In order to select the tephra layers that we would examine, we applied a sequence of criteria. Firstly, we excluded all layers < 2 mm thick because we considered it unlikely that such thin layers would have had an effect upon the palaeovegetation detectable using palynological techniques, given the extensive pollen catchment of LGdM. This excluded 183 of the total of 396 distinct tephra layers that have been identified in the sediments of LGdM (Fig 2.; Wulf, 2000). Secondly, we excluded 25 layers that had been identified as re-worked when the sediments were examined in thin section (Achim Brauer, pers. comm.). Thirdly, because we wished to ensure both that the vegetation present before the tephra was deposited had recovered from any previous episode of deposition and that sufficient time passed before deposition of the subsequent tephra layer for the vegetation to recover, we excluded 87 layers separated from the previous or subsequent layer by < 20 yr. Fourthly, of the 101 candidate tephra layers remaining, we excluded seven that were deposited during the mid- and late-Holocene when confounding impacts of human activities upon the vegetation could not be excluded. Finally, 29 of the 94 remaining candidates were in the earliest sediments recovered from the site; because these were recovered using a smaller diameter of corer than the later sediments, insufficient material was available to perform the required analyses. Of the

remaining 65 candidates, ten were selected for investigation, taking into account the issues we wished to address; Table 1 provides details of the characteristics of these ten layers.

Material for pollen analyses of the selected layers was obtained from cores collected during the 1990 (core D), 1993 (core J) and 1994 (core L) coring campaigns (led by colleagues from the University of Trier and subsequently GFZ-Potsdam, Germany). After collection each core section was split and one half of each was stored in Durham in the dark at 4°C, the other half being stored at GFZ-Potsdam. Most of the cores remain in excellent condition. High temporal resolution samples were taken immediately below and for some distance above each selected tephra layer. Where possible a 'miniature monolith', 400 mm^2 in cross section and spanning the tephra layer, was first cut from the core using a 'monolith box'. The monolith box was then inserted into a device developed at Durham University by J.R.G. Daniell that allows the sediment monolith to be extruded in suitably small increments. Samples of the required thickness were taken by slicing off extruded sections of the monolith using a scalpel. Where annual laminations were ≥ 1 mm in thickness sampling was guided by the laminations so as to attain annual sample resolution, thus avoiding sub-annual samples that could lead to sample-to-sample variations in pollen content related to the season(s) of the year represented. Where the laminations were obscure sampling interval was determined according to the inferred sediment accumulation rate, once again with the aim of obtaining annual samples, although the results obtained indicated that this was not always achieved. Where annual laminations were < 1 mm in thickness, however, samples of *ca*. 1 mm were taken and the number of annual laminations each spanned was estimated. This was necessitated not only because samples < 1 mm in thickness are very difficult to obtain, but also because thinner samples proved not to yield sufficient material for adequate pollen counts to be obtained. In all cases the thickness, number of years spanned and volume were recorded for each sample taken.

Pollen samples were prepared using standard techniques. Prior to treatment a measured volume of a suspension of known concentration of pollen of the exotic *Corymbia ficifolia* (formerly *Eucalyptus ficifolia*) was added to each sample so as to enable calculation of pollen accumulation rates (PARs). Initial treatment with hydrochloric acid (10%) was followed by treatment with sodium hydroxide (10%) before density separation of organic material using a saturated solution of zinc chloride (specific gravity 2·0). Washing with glacial acetic acid followed, before acetolysis, using a 9:1 mixture of acetic anhydride and concentrated sulphuric acid, and finally dehydration of the residues by repeated washing with 2-

methylpropan-2-ol ('tertiary butyl alcohol'). The residues were then suspended in silicone oil of 2000 cs viscosity and sub-samples mounted on microscope slides for pollen counting.

Pollen was examined and counted using a compound light microscope (Leica DM/LM); routine identifications and counting were performed at x400 magnification, with critical identifications made using a magnification of x1000. Identifications were made using published monographs and keys, supplemented where necessary by examination of specimens from the collection of pollen reference slides held by the Department of Biosciences, Durham University. Pollen data were entered and processed using Microsoft Excel®. PARs were calculated for each sample using the sediment accumulation rate for that sample derived from the annual lamination thicknesses and the proportions of fossil pollen and pollen of *C. ficifolia* counted in that sample. Pollen diagrams were prepared initially using Tilia Version 2.0.41 and refined using CorelDraw®.

Results

The pollen analytical results are presented as a series of pollen diagrams showing PARs, thus enabling tephra impacts that altered pollen productivity, either of individual taxa or of the vegetation generally, as well as those that impacted upon vegetation composition, to be identified. Age scales on the pollen diagrams have the year of tephra deposition as year zero. Pollen data are shown with a discontinuity that extends between the last sample analysed prior to tephra deposition and the first analysed after the tephra; in most cases this 'hiatus' spans no more than a few years. Pollen diagrams have been grouped according to the nature of the inferred regional vegetation present immediately prior to tephra deposition (Table 1(b)); vegetation inferences follow Allen *et al*. (2000). Thus, Figs. 4 and 5 present diagrams for five tephra layers deposited during periods when cold steppe vegetation predominated, Fig. 6 presents diagrams for three tephra layers deposited during periods with wooded steppe vegetation and Fig. 7 presents diagrams for two tephra layers deposited when temperate summergreen forest prevailed. The impacts recorded by the pollen diagrams are discussed below for each in turn of these three general vegetation types.

Cold steppe vegetation

Periods of inferred cold steppe were characterised by a predominance of pollen of herbaceous taxa, especially Poaceae, *Artemisia* and Chenopodiaceae. The principal woody plants represented consistently in the pollen spectra are *Pinus* subgen. *Pinus*, Cupressaceae and *Betula*, although a number of other tree taxa are also represented in some cases. The inferred climatic conditions indicate sub-zero mean temperatures of the coldest month of the year and marked moisture deficiency (Table 1(b); see also Supplementary Information Fig. S1).

TM-18-1d (Fig. 4(a)) was a relatively thin (20 mm) layer of basic chemistry (Table 1(a) and Supplementary Information Table S1; Wulf et al., 2006). It fell on vegetation dominated by steppic herbaceous taxa, especially Poaceae and *Artemisia*, although with moderate representation of *Pinus* subgen. *Pinus*, Cupressaceae and *Quercus robur*-type*,* along with sparse occurrences of other trees, including *Alnus*, *Abies* and *Fagus*. Although total PAR was initially reduced following the tephra fall, there was little longer-term impact upon the pollen productivity or composition of the vegetation, most pollen taxa having similar accumulation rates <*5* yr after the event to those preceding the event. A few taxa, however, notably *Fagus*, *Abies* and *Alnus*, showed reduced accumulation rates for a decade or so after the event.

TM-18 (Fig. 4(b)) in marked contrast was one of the thicker tephra layers examined (165 mm). It fell upon generally similar vegetation to that upon which TM-18-1d fell. Pollen productivity was generally somewhat reduced after the event, and did not recover to previous levels for *ca* 80 yr. There were also selective and persistent impacts upon a number of herbaceous and several woody plant taxa. Cyperaceae accumulation rate was much reduced and had not recovered 120 yr after the event. Other herbaceous taxa that showed persistently reduced accumulation rates include *Anthemis*-type, *Centaurea solstitialis*-type, *Plantago* and *Thalictrum*. Although Poaceae and *Artemisia* also showed some reduction in accumulation rates after the tephra fall, they, along with Chenopodiaceae, continued to dominate the pollen spectra as they did prior to the tephra fall. Woody taxa, some of which were relatively abundant prior to the tephra fall, generally had reduced accumulation rates following tephra deposition. The most abundant woody taxon prior to the tephra fall, *Pinus* subgen. *Pinus*, however, showed a less marked reduction in accumulation rate than most other woody taxa. This may indicate either that *Pinus* subgen. *Pinus* was much less impacted by the tephra than were the other woody taxa, or else that the pollen of

Pinus subgen. *Pinus* reaching LGdM at this time was derived principally from stands of *Pinus* subgen. *Pinus* sufficiently remote not to have been impacted by the tephra. Amongst the woody taxa that showed markedly reduced accumulation rates following deposition of the tephra, Cupressaceae, *Abies* and *Fagus* had not recovered to previous levels >100 yr after the event, whereas *Quercus robur*-type had recovered after *ca*. 60 yr and *Alnus* after *ca*. 80 yr.

TM-16b (Fig. 4(c)) was of intermediate thickness (66 mm) and, in contrast to TM-18-1d and TM-18 that are basic tephras, was chemically intermediate. Herbaceous taxa once again dominated prior to tephra deposition, especially Poaceae and *Artemisia*, although *Pinus* subgen. *Pinus*, Cupressaceae, *Betula* and *Quercus robur*-type were relatively abundant. Despite its thickness, this tephra fall apparently had only a very short-lived impact upon the vegetation. Accumulation rates of most taxa 2 – 3 yr after the event were comparable to those prior to the event, rising to a peak 3 – 5 yr after the event when total PAR was for a few years approximately double that prior to the event. This peak may reflect a fertilising effect of this chemically intermediate tephra resulting in more vigorous vegetation growth.

TM-15 (Fig. 5(a)) was the thickest of the tephra layers examined (325 mm) and was of basic chemistry. Its impact upon the vegetation was severe, with a very marked and persistent reduction in overall pollen productivity. The dominant herbaceous taxa, Poaceae, *Artemisia* and Chenopodiaceae, took *ca*. 50 yr before they showed any significant recovery, and even >100 yr after the event their accumulation rates were much reduced compared to those prior to the event. Accumulation rates of most other herbaceous taxa had returned to levels comparable to those prior to the event after *ca*. 50 yr. Accumulation rates of a minority of these herbaceous taxa that represent plant taxa many of which are of a ruderal character, notably Brassicaceae and Asteraceae subfam. Cichorioideae, reached levels markedly higher than prior to the event following their recovery *ca*. 50 yr after the event. Other taxa, such as *Helianthemum*, however, that represent longer-lived perennials typical of undisturbed grasslands, showed little recovery even > 100 yr after the event. The impact upon Cupressaceae, which was the dominant woody taxon prior to the event, was similarly persistent and very marked, with accumulation rates > 100 yr after the event mostly an order of magnitude less than before the event. Other woody taxa that were relatively abundant prior to the event, including *Pinus* subgen. *Pinus*, *Quercus robur*-type, *Alnus*, *Abies* and *Fagus*, also all showed

persistently reduced accumulation rates, with none having recovered to previous levels a century after the event.

TM-13 (Fig. 5(b)) was another relatively thick tephra layer (180 mm), but of intermediate chemistry. Its impact upon the vegetation was somewhat less marked than was that of either of the other relatively thick tephras that fell upon cold steppe vegetation, TM-18 and TM-15, both of which were of basic chemistry. Overall pollen productivity was substantially reduced by this tephra fall, with accumulation rates of a number of pollen taxa, including *Quercus robur*-type, *Fagus*, *Hippophaë*, Poaceae, Cyperaceae, *Anthemis*-type, *Helianthemum*, *Plantago* and *Rumex*-type, markedly reduced. A small number of taxa, however, had increased accumulation rates after the event, including *Cirsium*-type, *Androsace* and *Helleborus*-type. Cupressaceae, which was abundant before the event, had very markedly reduced accumulation rates after the event, as had Cyperaceae; in both cases the impact was persistent with accumulation rates showing no significant recovery >25 yr after the event.

Wooded steppe vegetation

Whilst herbaceous taxa, especially Poaceae and *Artemisia*, are abundant during the intervals characterised as wooded steppe, pollen of woody taxa is more abundant than during the periods of cold steppe vegetation, although still accounting for < 70% of the terrestrial pollen sum (Allen et al., 2000). Inferred climatic conditions differ from those during periods with cold steppe vegetation principally with respect to moisture deficiency, which is generally much less severe. Coldest month mean temperatures, although again generally sub-zero, are not as cold as during intervals with cold steppe vegetation.

TM-21-1a (Fig. 6(a)) Prior to the fall of this 20 mm thick tephra the principal components of the pollen spectra derived from woody plants were *Pinus* subgen. *Pinus*, *Quercus robur*-type, *Alnus* and *Abies*, with lesser but consistent amounts of Cupressaceae, *Fagus*, Ulmaceae and *Betula*. Poaceae was the single most abundant taxon, with *Artemisia* the next most abundant herbaceous pollen taxon. Several other herbaceous taxa, including Chenopodiaceae, *Anthemis*-type and Brassicaceae, were consistently present at moderate accumulation rates. After deposition of the tephra all pollen taxa showed a marked reduction in PARs. Furthermore, despite the tephra layer being one of the thinner of those examined (20 mm), the marked reduction in accumulation rates was persistent, with only a minority of taxa showing any significant recovery after 90 yr. Those taxa which did show some recovery by that time were several of the

broadleaved summergreen trees, notably *Quercus robur*-type, *Alnus* and *Fagus*. In contrast, others of this functional type, notably *Betula*, were essentially absent during the nine decades following the tephra fall, and most of the herbaceous taxa also showed little recovery. One feature shown by many of the taxa, however, was a short-lived peak of higher PARs *ca*. 10 yr after the tephra fall. Given the time elapsed between tephra deposition and this peak, and that the relative abundances of taxa do not closely match those in the pre-tephra pollen spectra, this peak may reflect a short-lived fertilising effect of the tephra as it weathered.

TM-18-13 (Fig. 6(b)) was the thinnest of the tephra layers examined at just 5 mm. The vegetation upon which it fell had Poaceae, along with *Artemisia* and Chenopodiaceae, as the most abundant herbaceous pollen taxa and *Quercus robur*-type, along with *Pinus* subgen. *Pinus*, *Abies*, *Betula* and *Fagus*, as the most abundant pollen taxa derived from woody plants. Overall the pollen spectra were diverse, with a large number of both herbaceous and woody plant taxa represented. PARs generally were unchanged following deposition of the tephra; the diversity of pollen taxa was also more or less unaltered.

TM-17-2 (Fig. 6(c)) is another of the thinner tephra layers investigated (30 mm), although it nonetheless had a very substantial impact upon the vegetation. Overall PAR after the tephra fall was reduced by >99%, more than following any of the other tephra falls investigated. Prior to the tephra fall the most abundant herbaceous taxa were Poaceae and *Artemisia*, accompanied by relatively high abundances of Cyperaceae and Chenopodiaceae with a range of other taxa also represented. The most abundant pollen taxa representing woody plants were *Pinus* subgen. *Pinus*, Cupressaceae and *Quercus robur*-type, with lesser amounts of pollen of *Fagus* and *Ostrya*-type. Following deposition of the tephra PARs of almost all taxa were very markedly reduced, the most noticeable exception being Asteraceae subfam. Cichorioideae, accumulation rates of which increased and persisted at higher levels than before until *ca*. 30 yr after the tephra fall, at which time accumulation rates of many taxa showed their first signs of recovery, albeit still only to levels markedly less than before the tephra fall. In addition to the taxa present prior to tephra deposition, several pollen taxa representing herbaceous plants of a relatively ruderal character, including Brassicaceae and *Rumex*-type, that were essentially absent prior to tephra deposition also showed increased accumulation rates at this time.

Forest vegetation

During the intervals characterised as having forest vegetation, pollen derived from trees accounted for > 70% of the pollen of terrestrial plants. Although the composition of the pollen spectra, and hence of the forests, differed between the two tephra falls during forest periods that we investigated, the dominant functional type was the broadleaved summergreen tree, with *Quercus robur*-type the most abundant pollen taxon associated with this functional type. Amongst the pollen taxa representing herbaceous plants, Poaceae was the most abundant taxon. The inferred climatic conditions were markedly different from those of either the cold steppe or wooded steppe periods. In particular, moisture deficiency was markedly less even than during the periods with wooded steppe vegetation. Winter temperatures were also higher, with the median reconstructed value for coldest month mean temperature being > 0° C for both tephra layers investigated.

TM-24a (Fig. 7(a)) was a relatively thick basic tephra layer (70 mm) that had a substantial impact upon the vegetation. Prior to the tephra fall the most abundant pollen taxon was *Quercus robur*-type, along with *Fagus*, *Alnus*, *Abies*, Ulmaceae, *Carpinus betulus* and *Ostrya*-type. Poaceae was markedly the most abundant of the pollen taxa representing herbaceous plants. Following deposition of the tephra, PARs were markedly reduced for > 25 yr, although with a short-lived peak during the first 5 yr after tephra deposition. The composition of this peak, however, mirrors the composition of pollen spectra prior to deposition, which likely indicates that in this case the peak represents re-deposition of pollen derived from soils or surficial marginal lake sediments exposed to erosion as a result of a reduction in vegetation cover resulting from the tephra fall. When PARs largely returned to their previous levels, *ca*. 25 yr after the tephra fall, there was little or no evidence of any change in composition of the vegetation. Interestingly, there also was no evidence of earlier recovery of more light-demanding tree taxa, suggesting that the recovery was not primarily by recolonization or regeneration from seeds but instead involved either re-sprouting or recovery of damaged individuals.

TM-6b (Fig. 7(b)) was another relatively thick tephra layer (106 mm), but of an intermediate rather than of a basic chemistry. Prior to its deposition the dominant pollen taxa representing trees were *Quercus robur*-type, *Alnus*, *Corylus* and *Ostrya*-type, with lesser quantities of a range of other taxa. Poaceae was the dominant pollen taxon representing herbaceous plants. Anomalously, PARs were generally increased

following deposition of this tephra, and this increase occurred immediately with no lag. Furthermore, the composition, in terms of the taxa present and their relative abundances, of the pollen spectra immediately following deposition of the tephra did not differ substantially from that of the spectra preceding the tephra. It thus appears that deposition of this relatively thick tephra had limited impact upon the vegetation. The lower PAR before and persistent general increase in PAR following tephra deposition may be accounted for by the short-lived minimum in moisture availability that more or less coincides with the tephra layer (Supplementary Information, Fig. S1). It should be noted here that the reconstruction of climatic conditions from the pollen data uses only the relative abundances of a sub-set of taxa (Parnell et al., 2016) and takes no account of PARs.

Discussion

Our results allow us to assess each of our expectations, and to reach a number of conclusions about the impacts of past tephra falls in southern Italy. With respect to our expectation that episodes of tephra deposition during the late-Pleistocene caused disturbance of vegetation structure and composition in the landscape surrounding Lago Grande di Monticchio, our results generally provide support. In eight of the ten cases examined PARs were reduced, often markedly so, after tephra deposition, probably indicating a marked reduction in vegetation productivity most likely accounted for by major disturbance to the vegetation, and hence reduced vegetation cover. In half of these cases there was also evidence of marked changes in vegetation composition after tephra deposition. Although in one case (TM-18-13) there was essentially no change in productivity or composition after tephra depositions, this was the thinnest layer examined at just 5 mm. The only notable example of a tephra layer not conforming to this hypothesis was TM-6b, deposited during the early Holocene, deposition of which coincided with a marked increase in PAR. This anomalous case, however, is most likely accounted for by the impact upon vegetation productivity of a change in moisture availability, from much drier conditions prior to the tephra fall to moister conditions more favourable to the prevailing forest vegetation immediately following the tephra fall.

Our second expectation was that the magnitude and duration of the impact upon vegetation of an episode of tephra deposition was dependent upon the thickness of the tephra layer deposited, thicker layers

resulting in greater and more persistent impacts (cf. del Moral and Grishin, 1999, Zobel and Antos, 1997). Overall this proposition was strongly supported by our results. A linear regression of minimum time for recovery of the vegetation, following tephra deposition, on the thickness of the tephra layer, with the intercept set at zero because logically if no tephra is deposited then the time to recovery will be zero, had a slope of 0·293 yr mm^{-1} and explained > 60% of the pattern in the data (r^2 = 0·604, F = 13·70, d.f. = 1, 9, p = 0·006). Nonetheless, tephra chemistry also influenced the duration of the impact, the three tephras of intermediate chemistry having much the largest negative residuals, indicating that for a given thickness of tephra layer vegetation recovered much more rapidly if the tephra was of intermediate rather than of basic chemistry (see Supplementary Information Fig. S2). This result is supported by the slope of 0·360 yr mm^{-1} obtained when performing an equivalent regression for just the seven basic tephras. The higher proportion (*ca*. 70%) of the pattern in these data that this regression explained (r^2 = 0·695, F = 13·67, d.f. = 1, 6, p = 0·014) also indicates that tephra chemistry has some influence, although this appears to be much weaker than that of tephra thickness.

Our third expectation was that the magnitude and duration of the impact upon vegetation of an episode of tephra deposition was dependent upon the general character of the vegetation present prior to tephra deposition. We expected herb-dominated vegetation to suffer greater and more enduring impacts from deposition of a given thickness of tephra than vegetation comprising a mixture of trees and herbaceous taxa or forest vegetation, the latter being expected to suffer least impact. Although we had limited sample numbers for each individual vegetation type, there was nonetheless clear evidence of differential sensitivity, as we had expected, at least in terms of the duration of the impact. However, the order of relative sensitivity was not that which we predicted. Instead it was the wooded steppe, a mixture of trees and herbaceous vegetation, that apparently was most sensitive to tephra deposition, with a strongly positive mean residual of *ca*. 35 yr in the regression of minimum time to recovery on tephra thickness Furthermore, inspection of Fig. S2 suggests a much more persistent effect of tephra falls on this vegetation type; the slope of a least-squares line through the origin fitted to just the three points for this vegetation type was around seven times steeper than the overall regression line. In contrast the five cold steppe samples had a mean residual of *ca*. -2 yr and a least-squares line through the origin fitted to these samples had a slope almost identical to that of the overall regression. Although we had only two samples representing forest vegetation, they had a mean residual of *ca*. -13 yr and a least-squares line through the

origin fitted to these samples had a slope almost three times shallower than that of the overall regression. Thus our results offer some support for our expectation that forest vegetation would be the least sensitive of the three vegetation types examined.

We used two further approaches to assess the magnitude, as opposed to the persistence, of the impacts of tephra deposition upon the vegetation. Firstly, we expressed the overall PAR for the first two samples following tephra deposition relative to overall PAR for the sample(s) shortly preceding the tephra. This assessment thus focused upon the extent to which overall pollen productivity, and hence by inference probably also overall vegetation productivity, was impacted by tephra deposition. Although the expected general negative relationship between relative PAR and tephra thickness was found, the relationship was weak, a large amount of variation in relative PAR clearly not being related to tephra thickness (see Supplementary Information Fig. S3). In terms of the three vegetation types, wooded steppe and cold steppe showed similar average magnitudes of impact using this assessment, mean PAR after tephra deposition being 33% and 35%, respectively, of that prior to deposition, although for a given thickness of tephra wooded steppe tended to show a greater magnitude of impact than cold steppe. A mean value was not computed for forest vegetation because of the confounding effects of climatic change upon the results of this assessment for one of the two tephra layers with this vegetation type; however, the relative PAR for the second tephra layer was only *ca*. 17%, indicating a very substantial impact upon the forest vegetation at that time. This very substantial reduction in overall PAR, as well as the substantial mean reductions for both cold steppe and wooded steppe samples, indicates that the majority of tephra deposition events caused marked disturbance regardless of vegetation type.

Our second approach to assessing the magnitude of the impacts focused primarily upon changes in vegetation composition. For each tephra layer we calculated the Euclidean Distances between the mean pollen spectrum for samples prior to deposition of the tephra and each sample following tephra deposition, pollen spectra being expressed in terms of the accumulation rates of the pollen taxa present. Unstandardised data were used because we wished to focus upon the impacts on the principal taxa present. In order to compare between tephras we normalised the Euclidean Distances for each tephra relative to the minimum and maximum values for samples following the tephra, thus obtaining values for each tephra that ranged between zero and one. Finally we took the mean normalised unstandardized

Euclidean Distance for the first two samples above each tephra. As expected, there was a pronounced positive relationship between these values and tephra thickness, thicker tephra layers on average being associated with more substantial changes in vegetation composition immediately following the deposition event. Despite greater variability in the impact of thinner, as opposed to thicker, tephra layers, a linear regression of mean normalised unstandardized Euclidean Distance on tephra thickness accounted for *ca*. 40% of variation in the former (r^2 = 0·398, F = 5·29, d.f. = 1, 8, p = 0·051; see Supplementary Information Fig. S4) The overall average of the mean normalised unstandardized Euclidean Distance values across all ten tephras was 0·514. Average values for the three vegetation types were: cold steppe – 0·572; wooded steppe – 0·497; and forest – 0·396, although there was considerable variation in each case, primarily related to tephra thickness. The mean residuals in the regression (cold steppe – -0·039, wooded steppe – 0·130 and forest – -0·098) indicate that deposition of a given thickness of tephra generally had greatest impact upon vegetation composition when the vegetation was wooded steppe and least impact upon forest.

These assessments of the persistence and magnitude of the impacts of tephra deposition clearly indicate the expected differential sensitivity of different vegetation types. However, the greatest sensitivity of wooded steppe vegetation, in terms both of the minimum time taken for the vegetation to recover after an episode of tephra deposition and the change in vegetation composition immediately following tephra deposition, was contrary to our expectations and is not readily explained. It is possible, however, that the composition of both the tree and herbaceous components of the vegetation differed from those of the cold steppe and forest types more than is suggested by the pollen records. Many of the pollen taxa that were recorded from all three vegetation types represent sub-genera (e.g. *Pinus* subgen. *Pinus*, Quercus robur-type), genera (e.g. *Artemisia*, *Alnus*), sub-families (e.g. Asteraceae subfam. Cichorioideae) or even families (e.g. Poaceae, Chenopodiaceae), comprising in some cases large numbers of ecologically distinct species. It may thus be that the herbaceous species, as well as the trees, comprising the wooded steppe vegetation suffered more enduring impacts of tephra deposition than did their related species that comprised the cold steppe vegetation because the former were inherently more sensitive. Such differential sensitivity is consistent with the likelihood that the cold steppe vegetation, dominated by herbaceous taxa, experienced more frequent disturbance episodes, especially associated with fires but also perhaps with extreme climatic events, than did the wooded steppe. The much greater abundance of trees in the latter is in itself probably

indicative of less frequent disturbance. The plant species comprising the cold steppe vegetation may thus be well-adapted to frequent disturbance and hence, as a result, able to recover relatively rapidly after an episode of tephra deposition, whereas the species associated with wooded steppe arguably are likely to be adapted to less frequent disturbances from which the vegetation then takes longer to recover.

Another unexpected result was the particular sensitivity of Cupressaceae, both in terms of the reduction in its PAR and the duration of the impact; this was seen especially in the case of some of the thicker tephra falls on cold steppe vegetation, notably TM-18, TM-15 and TM-13. It is most likely that this pollen taxon represents one or more species of *Juniperus*, although neither *Cupressus sempervirens* nor *Tetraclinis articulata* can definitely be ruled out. Of the several candidate *Juniperus* spp. that may have occurred in association with cold steppe vegetation, the most likely is perhaps *J. sabina* that is widespread today from western Europe to the Russian Far East and occurs not only in montane habitats but also in *Artemisia* steppes and desert areas of Central Asia (Farjon, 2013). In common with other likely species this is a scale-leaved species amongst whose foliage tephra will likely accumulate more readily than in the case of needle-leaved species. In contrast to the other likely species that mostly form tall shrubs or low trees, for example *J. excelsa*, *J. sabina* is typically very low-growing and mat forming, which is also likely to increase its sensitivity to deposition of relatively thick tephra layers.

The considerable variation in the duration of the impacts of the tephra deposition events, and the relationship between this and tephra thickness, likely reflects qualitatively different mechanisms of impact depending upon the depth of tephra deposited. Recovery of woody vegetation components within only a few years after deposition of thinner tephra layers indicates that they suffered only a temporary setback, perhaps as a result of defoliation caused by the tephra. Similarly rapid recovery of herbaceous components, however, might indicate either re-sprouting from perennating organs or re-colonisation by dispersing propagules. Given that tephra deposition events, however, were almost certainly geographically extensive, such rapid re-colonisations would only be possible if patches of vegetation survived the tephra deposition event in local enclaves that were protected from tephra deposition. Longer recovery periods of one to a few decades associated with moderate depths of tephra deposition may reflect woody plants either re-sprouting or re-colonising by dispersing propagules, although the lack of evidence of earlier re-colonisation by more light-demanding taxa suggests that re-sprouting was more important. In

general angiosperm taxa are more often able to re-sprout, whereas gymnosperm taxa are less often capable of this. The particularly marked impact upon Cupressaceae discussed above thus may reflect the inability of many *Juniperus* spp. to re-sprout after a severe disturbance that destroys their canopy. In the case of herbaceous taxa, burial by moderate tephra accumulations likely killed most and recovery would be by re-colonisation by dispersing propagules. Such re-colonisation was almost certainly the dominant mechanism of recovery for both woody and herbaceous taxa in the case of thicker tephra deposits with minimum recovery times of many decades to a century or more.

In conclusion, our investigations not only provide evidence that strongly supports our expectations, but also reveal evidence of unexpected patterns of differential sensitivity to tephra deposition of both some individual plant taxa and of different vegetation types. Furthermore, these investigations demonstrate the considerable potential both of late-Quaternary sedimentary records and of palaeoecological methods in relation to investigating ecological processes that take place on timescales of years to a century or more. Whilst high temporal resolution sampling remains too labour intensive to be applied to the centennial to millennial time scales addressed by the majority of studies of Quaternary palaeoecology, it is a powerful approach for the investigation of phenomena such as those addressed here.

Authors' Contributions

BH conceived the project, designed the methodology and took the lead on drafting the manuscript; JRMA performed the pollen analyses, processed the resulting data and prepared the pollen diagrams; BH & JRMA together finalised the manuscript.

Acknowledgements

Research was supported by Leverhulme Trust project grant F/00 128/AV. We are grateful to Jörg Negendank, Achim Brauer and their colleagues at GeoForschungsZentrum, Potsdam, for making available sediment from cores collected at Lago Grande di Monticchio and for providing chronological data for these cores, and to Sabine Wulf for access to her data relating to the tephra layers in the cores. Paul Adam collected and supplied the pollen of *Corymbia ficifolia*. We are grateful to Matt McGlone and two anonymous reviewers for their helpful comments on our initial submission.

Data Accessibility

Pollen and chronological data are archived in the Neotoma Paleoecology Database (https://www.neotomadb.org/).

References

Aiuppa, A., Bellomo, S., Brusca, L., D'Alessandro, W., Di Paola, R. & Longo, M. (2006) Major-ion bulk deposition around an active volcano (Mt. Etna, Italy). *Bulletin of Volcanology,* **68,** 255-265.

Allen, J. R. M. & Huntley, B. (2009) Last interglacial palaeovegetation, palaeoenvironments and chronology: A new record from Lago Grande di Monticchio, southern Italy. *Quaternary Science Reviews,* **28,** 1521-1538.

Allen, J. R. M., Watts, W. A. & Huntley, B. (2000) Weichselian palynostratigraphy, palaeovegetation and palaeoenvironment: the record from Lago Grande di Monticchio, southern Italy. *Quaternary International,* **73/74,** 91-110.

Allen, J. R. M., Watts, W. A., McGee, E. & Huntley, B. (2002) Holocene environmental variability - the record from Lago Grande di Monticchio, Italy. *Quaternary International,* **88,** 69-80.

Antos, J. A. & Zobel, D. B. (2005) Plant responses in forests of the tephra-fall zone. *Ecological responses to the 1980 eruption of Mount St Helens* (eds V. H. Dale, F. J. Swanson & C. M. Crisafulli), pp. 47-58. Springer, New York.

Arnalds, O. (2013) The Influence of Volcanic Tephra (Ash) on Ecosystems. *Advances in Agronomy, Vol 121* (ed D. L. Sparks), pp. 331-380. Elsevier Academic Press Inc, San Diego.

Bellomo, S., Aiuppa, A., D'Alessandro, W. & Parello, F. (2007) Environmental impact of magmatic fluorine emission in the Mt. Etna area. *Journal of Volcanology and Geothermal Research,* **165,** 87-101.

Birks, H. J. B. & Lotter, A. E. (1994) The impact of the Laacher See Volcano (11000 yr BP) on terrestrial vegetation and diatoms. *Journal of Paleolimnology,* **11,** 313-322.

Blackford, J. J., Edwards, K. J., Dugmore, A. J., Cook, G. T. & Buckland, P. C. (1992) Icelandic volcanic ash and the mid-Holocene Scots pine (*Pinus sylvestris*) pollen decline in northern Scotland. *The Holocene,* **2,** 260-265.

Brauer, A., Allen, J. R. M., Mingram, J., Dulski, P., Wulf, S. & Huntley, B. (2007) Evidence for last interglacial chronology and environmental change from Southern Europe. *Proceedings of the National Academy of Sciences,* **104,** 450-455.

Charman, D. J., West, S., Kelly, A. & Grattan, J. (1995) Environmental change and tephra deposition: The Strath of Kildonan, northern Scotland. *Journal of Archaeological Science,* **22,** 799-809.

Colombo, C., Sellitto, V. M., Palumbo, G., Di Iorio, E., Terribile, F. & Schulze, D. G. (2014) Clay formation and pedogenetic processes in tephra-derived soils and buried soils from Central-Southern Apennines (Italy). *Geoderma,* **213,** 346-356.

Daniell, J. R. G. (1997) *The late-Holocene palaeoecology of Scots Pine (Pinus sylvestris L.) in north-west Scotland*. Ph.D., University of Durham, Durham.

del Moral, R. & Grishin, S. Y. (1999) Volcanic disturbances and ecosystem recovery. *Ecosystems of Disturbed Ground* (ed L. R. Walker), pp. 137-160. Elsevier, Amsterdam.

Eastwood, W. J., Tibby, J., Roberts, N., Birks, H. J. B. & Lamb, H. F. (2002) The environmental impact of the Minoan eruption of Santorini (Thera): statistical analysis of palaeoecological data from Golhisar, southwest Turkey. *Holocene,* **12,** 431-444.

Egan, J., Fletcher, W. J., Allott, T. E. H., Lane, C. S., Blackford, J. J. & Clark, D. H. (2016) The impact and significance of tephra deposition on a Holocene forest environment in the North Cascades, Washington, USA. *Quaternary Science Reviews,* **137,** 135-155.

Ermice, A. (2017) A pedological case study of volcanoclastically impacted landscapes: The Vesuvian Avellino air-fall deposits, Southern Italy. *Catena,* **149,** 241-252.

Farjon, A. (2013) *Juniperus sabina*. *The IUCN Red List of Threatened Species 2013: e.T42249A2966599*.

Fischer, D. G., Antos, J. A., Grandy, W. G. & Zobel, D. B. (2016) A little disturbance goes a long way: 33-year understory successional responses to a thin tephra deposit. *Forest Ecology and Management,* **382,** 236-243.

Gear, A. J. & Huntley, B. (1991) Rapid changes in the range limits of Scots Pine 4000 years ago. *Science,* **251,** 544-547.

Hoblitt, R. P., Miller, C. D. & Scott, W. E. (1987) Volcanic hazards with regard to siting nuclear-power plants in the Pacific Northwest. pp. 197. United States Department of the Interior: Geological Survey, Vancouver, WA.

Horrocks, M. & Ogden, J. (1998) The effects of the Taupo Tephra eruption of c. 1718 BP on the vegetation of Mt Hauhungatahi, central North Island, New Zealand. *Journal of Biogeography,* **25,** 649-660.

Hotes, S., Grootjans, A. P., Takahashi, H., Ekschmitt, K. & Poschlod, P. (2010) Resilience and alternative equilibria in a mire plant community after experimental disturbance by volcanic ash. *Oikos,* **119,** 952-963.

Hotes, S., Poschlod, P., Takahashi, H., Grootjans, A. P. & Adema, E. (2004) Effects of tephra deposition on mire vegetation: a field experiment in Hokkaido, Japan. *Journal of Ecology,* **92,** 624-634.

Huntley, B., Daniell, J. R. G. & Allen, J. R. M. (1997) Scottish vegetation history: The Highlands. *Botanical Journal of Scotland,* **49,** 163-175.

Jensen, B. J. L., Pyne-O'Donnell, S., Plunkett, G., Froese, D. G., Hughes, P. D. M., Sigl, M., McConnell, J. R., Amesbury, M. J., Blackwell, P. G., van den Bogaard, C., Buck, C. E., Charman, D. J., Clague, J. J., Hall, V. A., Koch, J., Mackay, H., Mallon, G., McColl, L. & Pilcher, J. R. (2014) Transatlantic distribution of the Alaskan White River Ash. *Geology,* **42,** 875-878.

Lees, C. M. & Neall, V. E. (1993) Vegetation response to volcanic eruptions on Egmont volcano, New Zealand, during the last 1500 years. *Journal of the Royal Society of New Zealand,* **23,** 91-127.

Long, C. J., Power, M. J., Minckley, T. A. & Hass, A. L. (2014) The impact of Mt Mazama tephra deposition on forest vegetation in the Central Cascades, Oregon, USA. *Holocene,* **24,** 503-511.

Martinson, D. G., Pisias, N. G., Hays, J. D., Imbrie, J., Moore, T. C., Jr. & Shackleton, N. J. (1987) Age dating and the orbital theory of the ice ages: development of a high-resolution 0 to 300,000-year chronostratigraphy. *Quaternary Research,* **27,** 1-29.

Narcisi, B. (1996) Tephrochronology of a late Quaternary lacustrine record from the Monticchio Maar (Vulture Volcano, Southern Italy). *Quaternary Science Reviews,* **15,** 155-165.

Parnell, A. C., Haslett, J., Sweeney, J., Doan, T. K., Allen, J. R. M. & Huntley, B. (2016) Joint palaeoclimate reconstruction from pollen data via forward models and climate histories. *Quaternary Science Reviews,* **151,** 111-126.

Payne, R. & Blackford, J. (2005) Simulating the impacts of distal volcanic products upon peatlands in northern Britain: an experimental study on the Moss of Achnacree, Scotland. *Journal of Archaeological Science,* **32,** 989-1001.

Rasmussen, S. O., Bigler, M., Blockley, S. P., Blunier, T., Buchardt, S. L., Clausen, H. B., Cvijanovic, I., Dahl-Jensen, D., Johnsen, S. J., Fischer, H., Gkinis, V., Guillevic, M., Hoek, W. Z., Lowe, J. J., Pedro, J. B., Popp, T., Seierstad, I. K., Steffensen, J. P., Svensson, A. M., Vallelonga, P., Vinther, B. M., Walker, M. J. C., Wheatley, J. J. & Winstrup, M. (2014) A stratigraphic framework for abrupt climatic changes during the Last Glacial period based on three synchronized Greenland ice-core records: refining and extending the INTIMATE event stratigraphy. *Quaternary Science Reviews,* **106,** 14-28.

Scarciglia, F., Zumpano, V., Sulpizio, R., Terribile, F., Pulice, I. & La Russa, M. F. (2014) Major factors controlling late Pleistocene to Holocene soil development in the Vesuvius area (southern Italy). *European Journal of Soil Science,* **65,** 406-419.

Turney, C. S. M., Lowe, J. J., Davies, S. M., Hall, V., Lowe, D. J., Wastegard, S., Hoek, W. Z. & Alloway, B. (2004) Tephrochronology of Last Termination Sequences in Europe: a protocol for improved analytical precision and robust correlation procedures (a joint SCOTAV-INTIMATE proposal). *Journal of Quaternary Science,* **19,** 111-120.

Vacca, A., Adamo, P., Pigna, M. & Violante, P. (2003) Genesis of tephra-derived soils from the Roccamonfina volcano, south central Italy. *Soil Science Society of America Journal,* **67,** 198-207.

Wilmshurst, J. M. & McGlone, M. S. (1996) Forest disturbance in the central North Island, New Zealand, following the 1850 BP Taupo eruption. *Holocene,* **6,** 399-411.

Wulf, S. (2000) *Das tephrochronologische Referenzprofil des Lago Grande di Monticchio – Eine detaillierte Stratigraphie des süditalienischen explosiven Vulkanismus der letzten 100,000 Jahre*. Dr.rer.nat., Universität Potsdam, Potsdam.

Wulf, S., Brauer, A., Mingram, J., Zolitschka, B. & Negendank, J. F. W. (2006) Distal tephras in the sediments of Monticchio maar lakes. *La Geologia del Monte Vulture* (ed C. Principe), pp. 105-122. Dipartimento Ambiente, Territorio e Politichi della Sostenibilità, Regione Basilicata.

Wulf, S., Kraml, M., Brauer, A., Keller, J. & Negendank, J. F. W. (2004) Tephrochronology of the 100 ka lacustrine sediment record of Lago Grande di Monticchio (southern Italy). *Quaternary International,* **122,** 7-30.

Zdanowicz, C. M., Zielinski, G. A. & Germani, M. S. (1999) Mount Mazama eruption: Calendrical age verified and atmospheric impact assessed. *Geology,* **27,** 621-624.

Zobel, D. B. & Antos, J. A. (1997) A decade of recovery of understory vegetation buried by volcanic tephra from Mount St. Helens. *Ecological Monographs,* **67,** 317-344.

Zolitschka, B. & Negendank, J. F. W. (1996) Sedimentology, dating and palaeoclimatic interpretation of a 76.3 ka record from Lago Grande di Monticchio, southern Italy. *Quaternary Science Reviews,* **15,** 101-112.

Tables

Table 1 Characteristics of tephra layers examined

Table 1 Characteristics of tephra layers examined

(a)

Tephra	Age (yr BP)	Synonym(s)[1]	Source[1]	Volcanic event[1]	Chemistry[1]	Thickness[2] (mm)	Years since previous	Years until next	Mean sediment accumulation rate (mm yr^{-1})	
									before	after
TM-6b	9678	MT-2 / PL-9 / L4	Vesuvius	Mercato (Pomici Gemelle)	Intermediate	106 (D)	216	58	0·38	0·60
TM-13	19,282	MT-5 / PL-19 / L9	Vesuvius	Pomici di Base	Intermediate	180 (L)	1789	1306	1·67	0·71
TM-15	27,256	MT-6 / PL-21 / L10	Phlegrean Fields	Y-3	Basic	325 (J)	2664	1890	0·71	0·56
TM-16b	31,121	MT-7 / PL-26 / L11	Vesuvius	Codola (base)	Intermediate	66 (D)	709	884	0·95	1·00
TM-17-2	35,531	PL33	Phlegrean Fields ?	Schiava, C-9	Basic	30 (J)	1242	551	1·73	0·50
TM-18	36,773	MT-8 / PL-35 / L12	Phlegrean Fields	Campanian Ignimbrite, Y-5	Basic	165 (J)	70	1242	1·86	1·78
TM-18-1d	37,363	PL38	Phlegrean Fields	C-15, SMP1-a	Basic	20 (J)	223	304	0·18	0·29
TM-18-13	49,631	–	Procida-Vivara	unknown event	Basic	5 (J)	629	222	0·36	0·50
TM-21-1a	78,833	PL60	Phlegrean Fields	C-20	Basic	20 (J)	112	235	2·00	2·00
TM-24a	101,572	MT-10 / PL-71	Campanian	X-5 (Pumice fallout)	Basic	70 (J)	50	361	3·30	2·25

(b)

Tephra	PAZ[3]	Terrestrial[4]/MOI stage[5]	Vegetation[6]	Inferred climate[7]
TM-6b	1d	Holocene / 1	Temperate summergreen forest	MTCO (0·7) 4·5 (7·4)°C; GDD5 (2413) 2695 (3002) degree days; AET/PET (0·80) 0·88 (0·96).
TM-13	4	GS-2 / 2	Cold steppe	MTCO (-10·9) -4·1 (1·8)°C; GDD5 (1108) 1874 (2536) degree days; AET/PET (0·23) 0·39 (0·51).
TM-15	4	GS-4 / 2	Cold steppe	MTCO (-3·6) 0·7 (4·3)°C; GDD5 (2230) 2697 (3175) degree days; AET/PET (0·07) 0·15 (0·32).
TM-16b	5a	GS-6 (GS-5.2) / 3	Cold steppe	MTCO (-9·7) -5·3 (-0·2)°C; GDD5 (1947) 2424 (2846) degree days; AET/PET (0·52) 0·61 (0·70).
TM-17-2	5b	GI-8 (GS-8) / 3	Wooded steppe	MTCO (-8·6) -3·1 (2·3)°C; GDD5 (2031) 2574 (3067) degree days; AET/PET (0·43) 0·62 (0·76).
TM-18	6	GS-9 (GI-8a) / 3	Cold steppe	MTCO (-8·4) -3·2 (2·1)°C; GDD5 (1940) 2455 (2958) degree days; AET/PET (0·34) 0·45 (0·58).
TM-18-1d	6	GS-9 (GI-8c) / 3	Cold steppe	MTCO (-9·5) -4·5 (0·8)°C; GDD5 (1829) 2375 (2857) degree days; AET/PET (0·45) 0·56 (0·66).
TM-18-13	11	GI-14 / 3	Wooded steppe	MTCO (-7·3) -2·0 (3·1)°C; GDD5 (1512) 1968 (2469) degree days; AET/PET (0·70) 0·77 (0·85).
TM-21-1a	17c	GI-21 / 5a	Wooded steppe	MTCO (-7·8) -2·8 (2·3)°C; GDD5 (1947) 2403 (2850) degree days; AET/PET (0·65) 0·73 (0·81).
TM-24a	19b	St Germain I / 5c	Temperate summergreen forest	MTCO (-3·3) 1·2 (4·9)°C; GDD5 (2065) 2376 (2693) degree days; AET/PET (0·82) 0·90 (0·96).

[1] Synonymy for tephra layers follows Sabine Wulf (pers. comm.); the source and volcanic event with which each tephra is associated follow Wulf *et al*. (2006, 2004) and Sabine Wulf (pers. comm.); chemical analyses of the tephras are presented by Wulf *et al*. (2006, 2004).

[2] Thicknesses of tephra layers in the core from which samples were taken for pollen analysis; cores are indicated by the letters in parentheses.

[3] Pollen assemblage zones as recognised by Allen *et al.* (2000, 2002).

[4] Terrestrial stages within the last glacial stage identified tentatively by visual correlation of the pollen record with Greenland ice core stable oxygen isotope data (Rasmussen et al., 2014). Where this identification conflicts with the Greenland ice core chronology the chronologically matching stage is also indicated in parentheses.

[5] Marine oxygen isotope stages identified on the basis of the SPECMAP chronology (Martinson et al., 1987).

[6] Vegetation types were inferred using the modified 'biomisation' procedure of Allen *et al*. (2000).

[7] Inferred climatic conditions follow the reconstruction presented by Parnell *et al*. (2016, see also Supplementary Information Fig. S1). MTCO – mean temperature of the coldest month; GDD5 – annual thermal sum above 5°C; AET/PET – ratio of actual to potential evapotranspiration. Values given are the (5%) 50% (95%) values under the probability density function of reconstructed values for the century closest to the age of the tephra.

Figures

Figure 1: Map showing volcanic regions of Italy and location of Lago Grande di Monticchio

(a) The distribution in Italy and the surrounding region of volcanoes active currently or during the late Pleistocene and Holocene. The location of Lago Grande di Monticchio is indicated by the black star. Volcanic districts and individual volcanoes are indicated as follows: TU – Tuscany; Roman Province: VU – Vulsini Hills, CI – Cimini District (including Vico volcano), SA – Sabatini Volcanic District, AB – Alban Hills; Campanian Province: PO – Ponza Islands, RO – Roccamonfina, CF – Phlegrean Fields, SV – Vesuvius, IS – Ischia Island, PR – Procida-Vivara, MV – Monte Vulture; Aeolian and Sicilian District: US – Ustica Island, AO – Aeolian Islands, ET – Etna, PA – Pantelleria. (b) Local topographic map with bathymetry of Lago Grande di Monticchio and core locations. (Redrawn from Wulf et al., 2004)

Figure 2: Lago Grande di Monticchio – summary pollen diagram, chronology and tephra layers

Plotted using the independent chronology for the site that is based on the extensive presence of annual sediment laminations, the summary pollen diagram (left-hand panel) shows the relative abundance of pollen taxa representing woody (dark grey) *versus* herbaceous (light grey) plant taxa. Sub-categories in each are indicated by dashed lines and are from left to right: boreal woody taxa (*Betula*, *Pinus* and *Juniperus*); mesic/nemoral woody taxa; Mediterranean woody taxa; steppic taxa; Poaceae; and other herbaceous taxa. The right-hand panel shows the age and thickness of each of the 396 tephra layers; note that a log scale is used for thickness. Also indicated are the terrestrial stages, the marine oxygen isotope stages, and the positions, indicated by arrows, and identities of the ten tephra layers investigated.

Figure 3: Tephra layer TM-24a with laminated sediments below and above

Photograph of sediment from core J collected during the 1994 coring campaign at Lago Grande di Monticchio. The almost 10 cm thick TM-24a (MT-10 / PL-71) tephra layer and the under- and over-lying laminated sediments are clearly illustrated (Photograph by Jens Mingram, GeoForschungsZentrum, Potsdam).

Figure 4: Pollen diagrams spanning tephra layers deposited when cold steppe prevailed

High temporal resolution pollen diagrams spanning three tephra layers deposited during intervals when cold steppe vegetation prevailed: (a) TM-18-1d; (b) TM-18; and (c) TM-16b. Only the principal pollen taxa are shown; values plotted are pollen accumulation rate (PAR, grains cm^{-2} yr^{-1}). Note the different vertical scales and the changes in horizontal scale, the latter indicated by the differences in shading of the pollen profiles. Patterned secondary profiles represent a 10x magnification that is used to reveal changes in PAR when the values are small. Truncated extreme peak values are indicated numerically.

Figure 5: Pollen diagrams spanning tephra layers deposited when cold steppe prevailed

High temporal resolution pollen diagrams spanning two tephra layers deposited during intervals when cold steppe vegetation prevailed: (a) TM-15; and (b) TM-13. Only the principal pollen taxa are shown; values plotted are pollen accumulation rate (PAR, grains cm^{-2} yr^{-1}). Note the different vertical scales and the changes in horizontal scale, the latter indicated by the differences in shading of the pollen profiles. Patterned secondary profiles represent a 10x magnification that is used to reveal changes in PAR when the values are small.

Figure 6: Pollen diagrams spanning tephra layers deposited when wooded steppe prevailed

High temporal resolution pollen diagrams spanning three tephra layers deposited during intervals when wooded steppe vegetation prevailed: (a) TM-21-1a; (b) TM-18-13; and (c) TM-17-2. Only the principal pollen taxa are shown; values plotted are pollen accumulation rate (PAR, grains cm^{-2} yr^{-1}). Note the different vertical scales and the changes in horizontal scale, the latter indicated by the differences in shading of the pollen profiles. Patterned secondary profiles represent a 10x magnification that is used to reveal changes in PAR when the values are small. Truncated extreme peak values are indicated numerically.

Figure 7: Pollen diagrams spanning tephra layers deposited when forest prevailed

High temporal resolution pollen diagrams spanning two tephra layers deposited during intervals when forest vegetation dominated: (a) TM-24a; and (b) TM-6b. Only the principal pollen taxa are shown; values plotted are pollen accumulation rate (PAR, grains cm^{-2} yr^{-1}). Note the different vertical scales and the changes in horizontal scale, the latter indicated by the differences in shading of the pollen profiles. Patterned secondary profiles represent a 10x magnification that is used to reveal changes in PAR when the values are small.

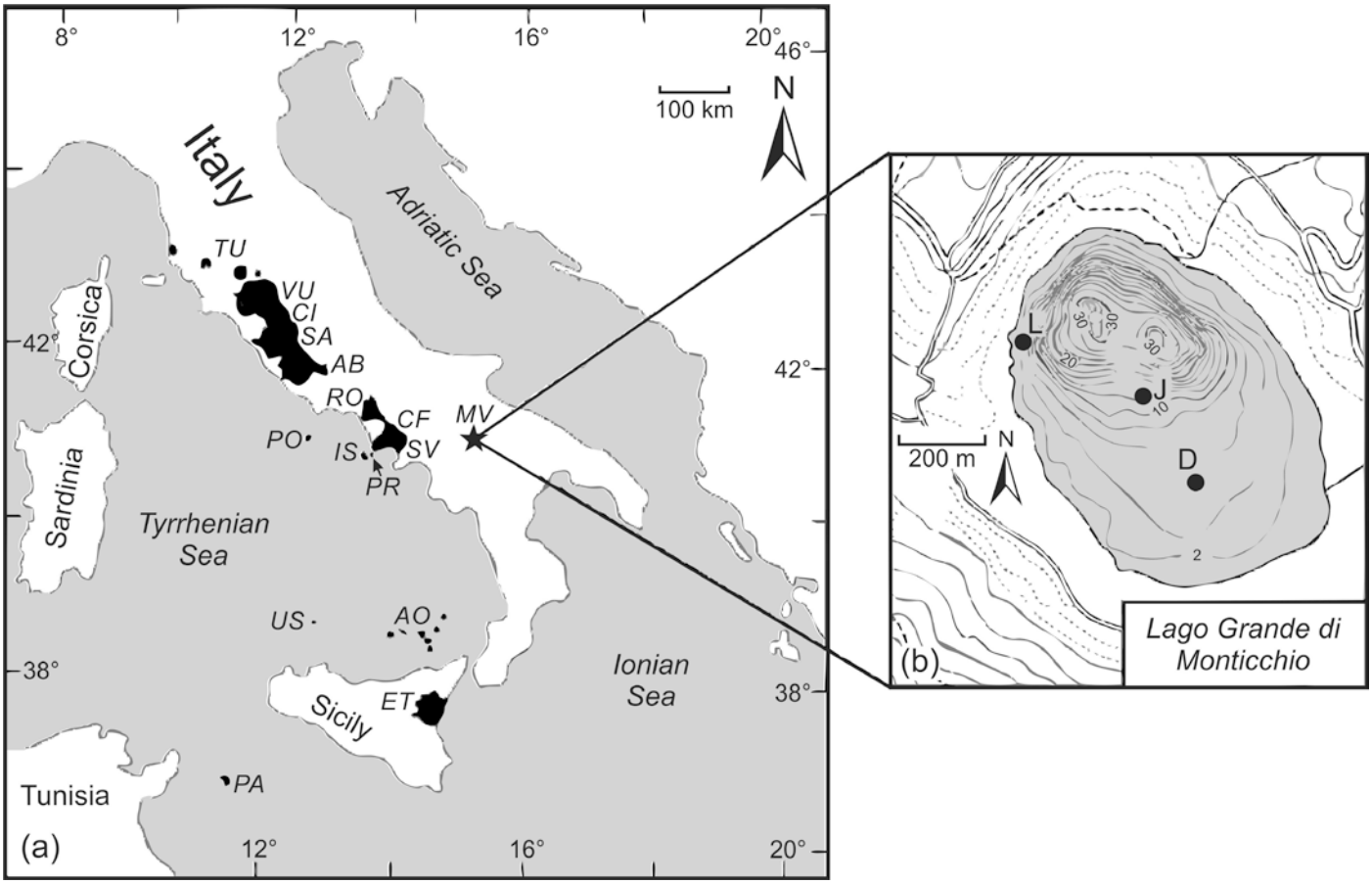

Figure 1: Map showing volcanic regions of Italy and location of Lago Grande di Monticchio

(a) The distribution in Italy and the surrounding region of volcanoes active currently or during the late Pleistocene and Holocene. The location of Lago Grande di Monticchio is indicated by the black star. Volcanic districts and individual volcanoes are indicated as follows: TU – Tuscany; Roman Province: VU – Vulsini Hills, CI – Cimini District (including Vico volcano), SA – Sabatini Volcanic District, AB – Alban Hills; Campanian Province: PO – Ponza Islands, RO – Roccamonfina, CF – Phlegrean Fields, SV – Vesuvius, IS – Ischia Island, PR – Procida-Vivara, MV – Monte Vulture; Aeolian and Sicilian District: US – Ustica Island, AO – Aeolian Islands, ET – Etna, PA – Pantelleria. (b) Local topographic map with bathymetry of Lago Grande di Monticchio and core locations. (Redrawn from Wulf et al., 2004)

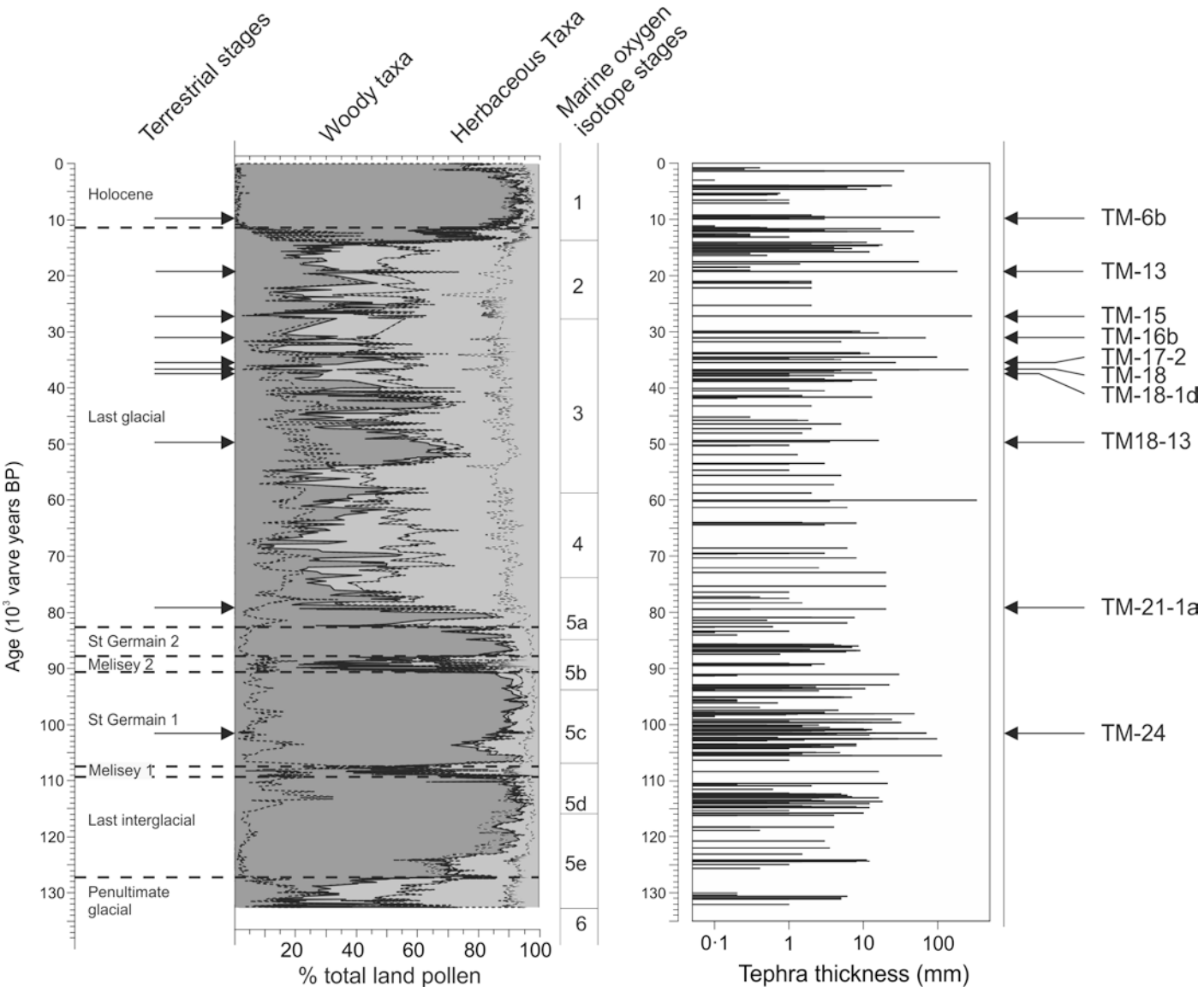

Figure 2: Lago Grande di Monticchio – summary pollen diagram, chronology and tephra layers

Plotted using the independent chronology for the site that is based on the extensive presence of annual sediment laminations, the summary pollen diagram (left-hand panel) shows the relative abundance of pollen taxa representing woody (dark grey) *versus* herbaceous (light grey) plant taxa. Sub-categories in each are indicated by dashed lines and are from left to right: boreal woody taxa (*Betula*, *Pinus* and *Juniperus*); mesic/nemoral woody taxa; Mediterranean woody taxa; steppic taxa; Poaceae; and other herbaceous taxa. The right-hand panel shows the age and thickness of each of the 396 tephra layers; note that a log scale is used for thickness. Also indicated are the terrestrial stages, the marine oxygen isotope stages, and the positions, indicated by arrows, and identities of the ten tephra layers investigated.

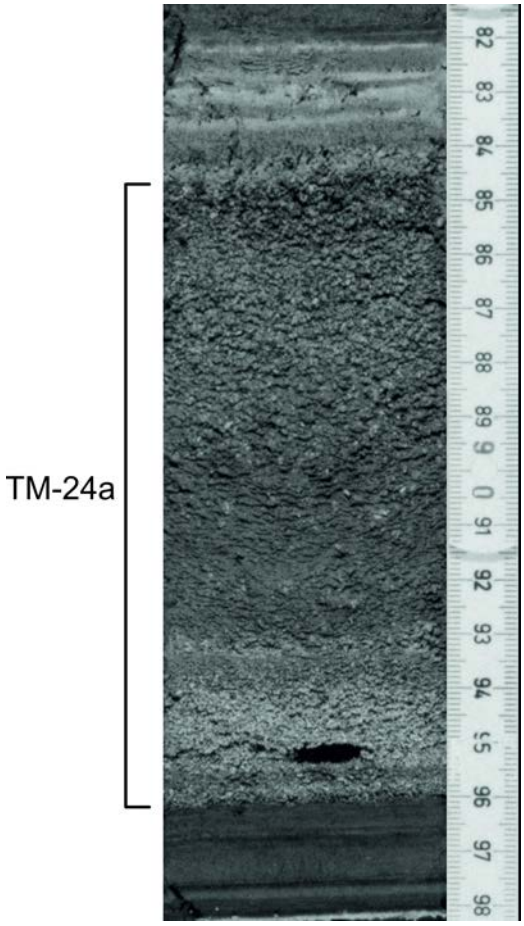

Figure 3: Tephra layer TM-24a with laminated sediments below and above

Photograph of sediment from core J collected during the 1994 coring campaign at Lago Grande di Monticchio. The TM-24a (MT-10 / PL-71) tephra layer and the under- and over-lying laminated sediments are clearly illustrated (Photograph by Jens Mingram, GeoForschungsZentrum, Potsdam.).

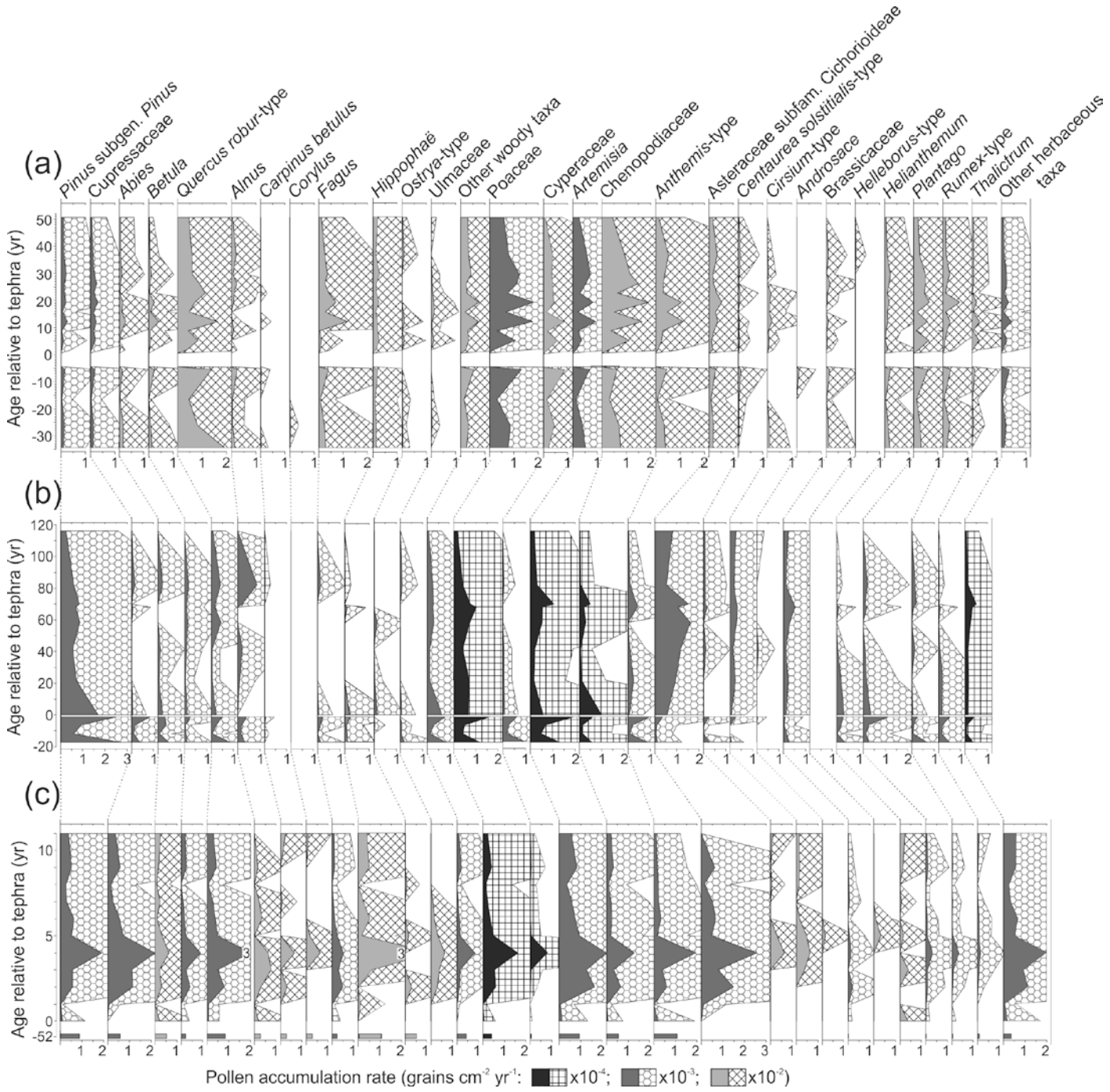

Figure 4: Pollen diagrams spanning tephra layers deposited when cold steppe prevailed

High temporal resolution pollen diagrams spanning three tephra layers deposited during intervals when cold steppe vegetation prevailed: (a) TM-18-1d; (b) TM-18; and (c) TM-16b. Only the principal pollen taxa are shown; values plotted are pollen accumulation rate (PAR, grains cm^{-2} yr^{-1}). Note the different vertical scales and the changes in horizontal scale, the latter indicated by the differences in shading of the pollen profiles. Patterned secondary profiles represent a 10x magnification that is used to reveal changes in PAR when the values are small. Truncated extreme peak values are indicated numerically.

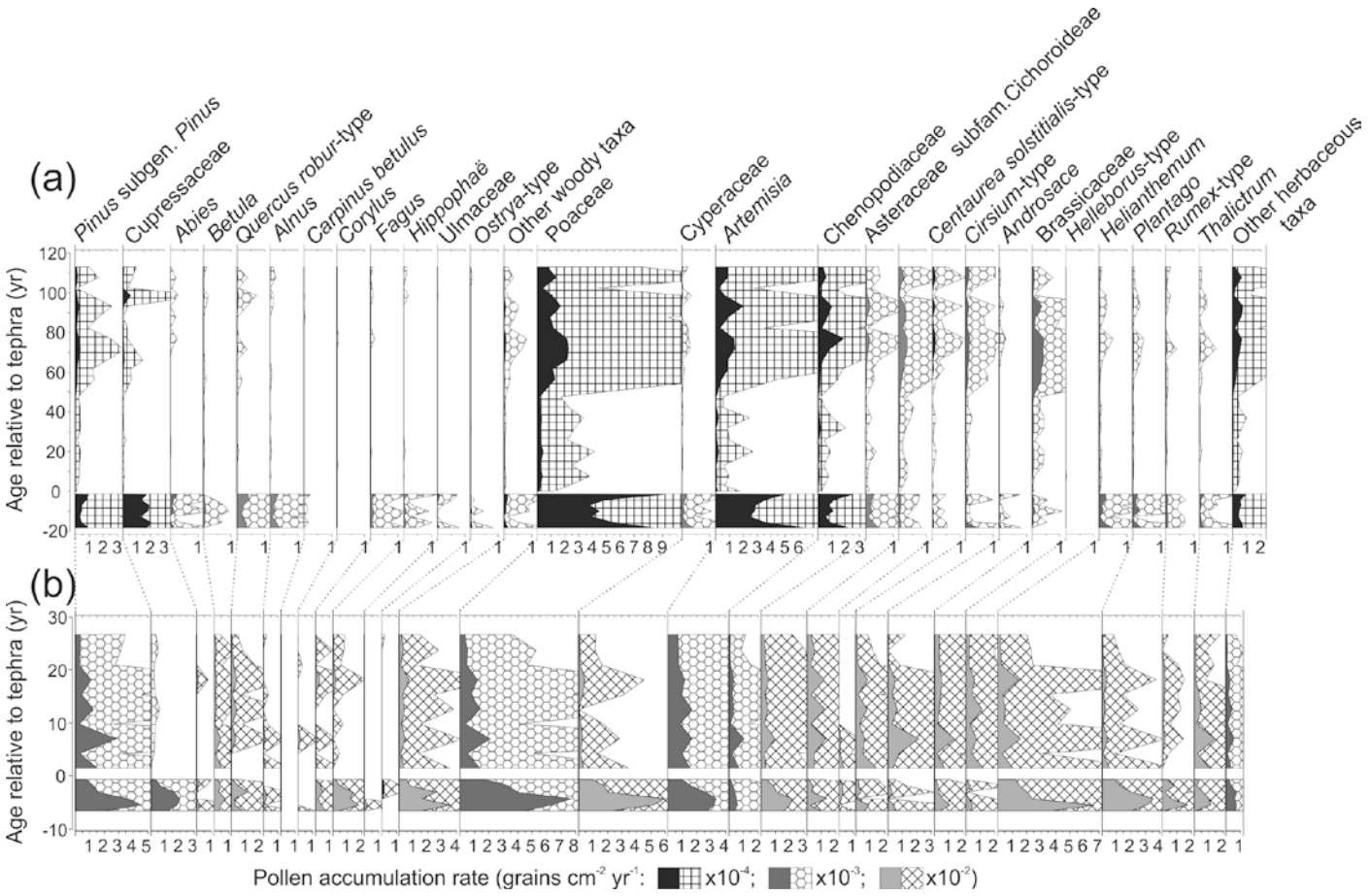

Figure 5: Pollen diagrams spanning tephra layers deposited when cold steppe prevailed

High temporal resolution pollen diagrams spanning two tephra layers deposited during intervals when cold steppe vegetation prevailed: (a) TM-15; and (b) TM-13. Only the principal pollen taxa are shown; values plotted are pollen accumulation rate (PAR, grains cm^{-2} yr^{-1}). Note the different vertical scales and the changes in horizontal scale, the latter indicated by the differences in shading of the pollen profiles. Patterned secondary profiles represent a 10x magnification that is used to reveal changes in PAR when the values are small.

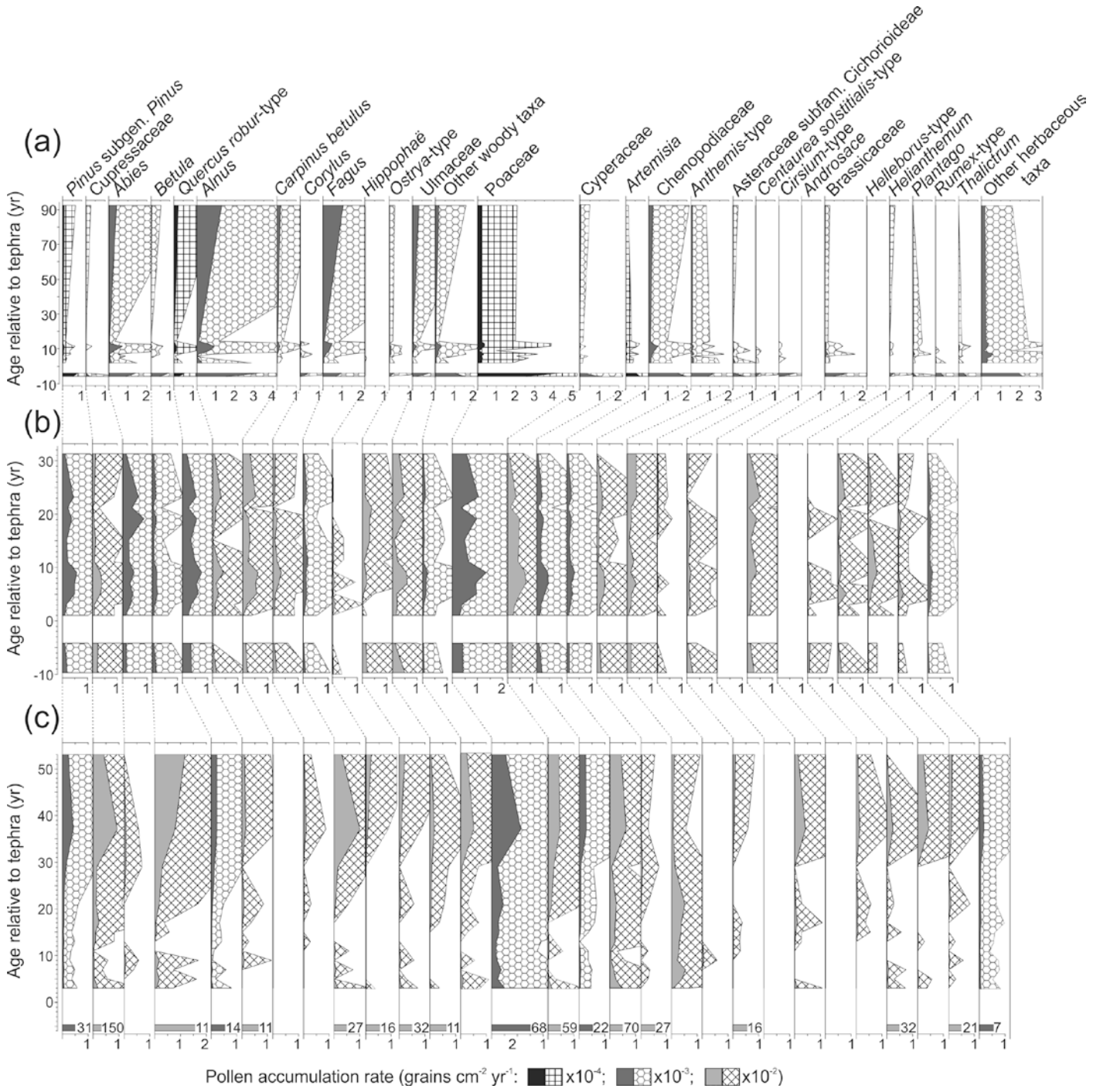

Figure 6: Pollen diagrams spanning tephra layers deposited when wooded steppe prevailed

High temporal resolution pollen diagrams spanning three tephra layers deposited during intervals when wooded steppe vegetation prevailed: (a) TM-21-1a; (b) TM-18-13; and (c) TM-17-2. Only the principal pollen taxa are shown; values plotted are pollen accumulation rate (PAR, grains cm^{-2} yr^{-1}). Note the different vertical scales and the changes in horizontal scale, the latter indicated by the differences in shading of the pollen profiles. Patterned secondary profiles represent a 10x magnification that is used to reveal changes in PAR when the values are small. Truncated extreme peak values are indicated numerically.

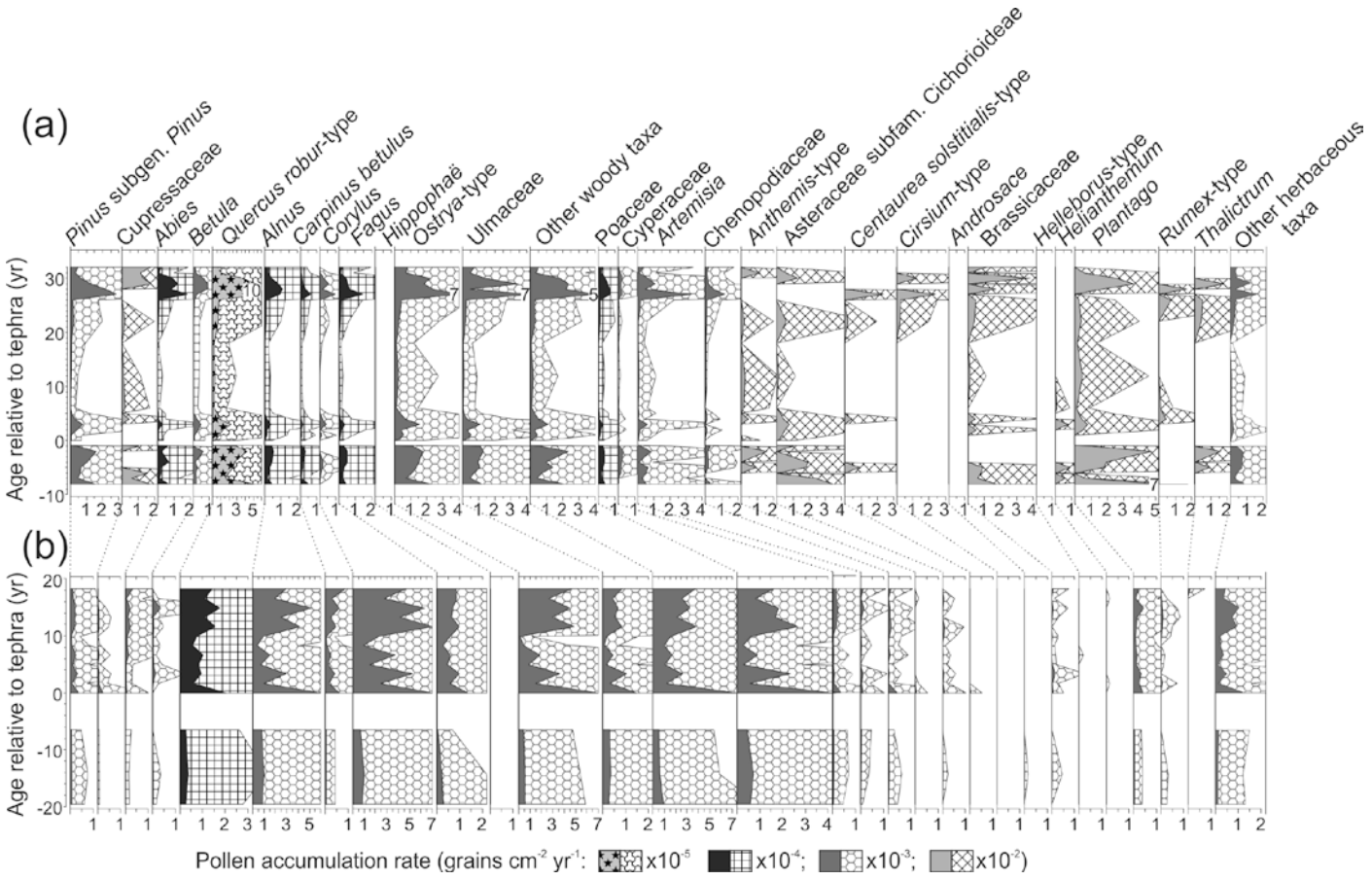

Figure 7: Pollen diagrams spanning tephra layers deposited when forest prevailed

High temporal resolution pollen diagrams spanning two tephra layers deposited during intervals when forest vegetation dominated: (a) TM-24a; and (b) TM-6b. Only the principal pollen taxa are shown; values plotted are pollen accumulation rate (PAR, grains cm^{-2} yr^{-1}). Note the different vertical scales and the changes in horizontal scale, the latter indicated by the differences in shading of the pollen profiles. Patterned secondary profiles represent a 10x magnification that is used to reveal changes in PAR when the values are small.